# UC Irvine
## UC Irvine Previously Published Works

### Title
Advances in Oral Cancer Detection Using Optical Coherence Tomography

### Permalink
https://escholarship.org/uc/item/36s0d2rm

### Journal
IEEE Journal of Selected Topics in Quantum Electronics, 11(4)

### ISSN
1077-260X

### Authors
Jung, Woonggyu
Zhang, Jun
Chung, Jungrae
et al.

### Publication Date
2005-08-01

### DOI
10.1109/jstqe.2005.857678

### Copyright Information
This work is made available under the terms of a Creative Commons Attribution License, available at https://creativecommons.org/licenses/by/4.0/

Peer reviewed

eScholarship.org Powered by the California Digital Library
University of California

# Advances in Oral Cancer Detection Using Optical Coherence Tomography

Woonggyu Jung, Jun Zhang, Jungrae Chung, Petra Wilder-Smith, Matt Brenner, J. Stuart Nelson, and Zhongping Chen, *Member, IEEE*

***Abstract*—Optical coherence tomography (OCT) is a new modality capable of cross sectional imaging of biological tissue. Due to its many technical advantages such as high image resolution, fast acquisition time, and noninvasive capabilities, OCT is potentially useful in various medical applications. Because OCT systems can function with a fiber optic probe, they are applicable to almost any anatomic structures accessible either directly, or by endoscopy. OCT has the potential to provide a fast and noninvasive means for early clinical detection, diagnosis, screening, and monitoring of precancer and cancer. With an imaging depth range of 2–3 mm, OCT diagnostics are particularly suitable for the oral mucosa. Currently, it is difficult to detect premalignant and malignant oral lesions due to their often multifocal nature and need for repeated biopsies.**

**The goal of this study was to evaluate the feasibility of OCT for the diagnosis of multiple stages of oral cancer progression. In this paper, we present not only conventional 2-D OCT images, but also 3-D volume images of normal and precancerous lesions. Our results demonstrate that OCT is a potential tool for cancer detection with comprehensive diagnostic images.**

***Index Terms*—3-D image, optical coherence tomography (OCT), oral cancer detection.**

## I. Introduction

FIFTEEN million people worldwide will be diagnosed with oral cancer this year [1], [2]. Cancer cure and survival relate directly to the stage of the cancer at the time of diagnosis. Early detection permits minimally invasive treatment and greatly improves long-term survival. In anatomical sites such as the oral cavity, early recognition of malignancy is problematic due to the frequent lack of gross signs or obvious symptoms. In many cases, detection is further hampered by poor visual access, difficulty in determining which of the commonly encountered dysplastic regions will transform into malignancy, and the inability to perform adequate or regularly repeated screening in high risk patients. Thus, a novel modality for the detection of oral malignancy is urgently needed.

Claiming approximately 10,000 lives annually in the U.S., oral squamous cell carcinoma is usually preceded by dysplasia presenting as white epithelial lesions or leukoplakia on the mucosa. Malignant transformation occurs unpredictably in up to 40% of patients over a five year followup. Cancer detection is further complicated by field cancerization which leads to multicentric lesions. Current diagnostic techniques require repeated surgical biopsy of benign lesions, yet they often detect malignant change too late for curative treatment. Of all oral cancer cases documented by the National Cancer Institute, advanced lesions outnumbered localized lesions at the time of diagnosis by more than 2:1, partly because many clinicians do not routinely inspect their patients for oral lesions, and partly due to the lack of effective diagnostic modalities. The five year survival rate is only 16% for patients with oral cancer metastasis, but 75% for those with localized disease at the time of diagnosis [1], [2].

In order to detect the transformation of leukoplakia to squamous cell carcinoma, various methods such as oral brush cytology, spectroscopy, and confocal reflectance microscopy have been used. "Brush biopsy" has been shown to provide moderate sensitivity levels of detection of oral epithelial dysplasia or squamous cell carcinoma, but poor specificity. Thus, this approach is of limited diagnostic value without augmentation by traditional biopsy [3]–[5]. Spectroscopy contains information about the biochemical composition and/or the structure of the tissue which conveys diagnostic information. Malignancy related biochemical and morphologic changes perturb tissue absorption, fluorescence, and scattering properties. Thus, biochemical information can be obtained by measuring absorption/reflectance, fluorescence, or Raman scattering signals. Structural and morphological information may be obtained by techniques that assess the elastic scattering properties of tissue [6], [7]. However, significant challenges to the use of diagnostic spectroscopy include the often low signal-to-noise ratio, difficulty in identifying the precise source of signals, data quantification, and establishing definitive diagnostic milestones and endpoints. *In vivo* confocal imaging resembles histological tissue evaluation, except that three-dimensional subcellular resolution is achieved noninvasively and without stains. In epithelial structures, resolutions of 1 $\mu$m have been achieved with a 200–400-$\mu$m field of view [8]–[10]. While this technology can provide detailed images of tissue architecture and cellular morphology, the very

Manuscript received January 14, 2005; revised June 30, 2005 and July 6, 2005. This work was supported by research grants awarded from the National Science Foundation (BES-86924), California Tobacco Related Disease Research Program (14IT-0097), and National Institutes of Health (EB-00255, NCI-91717, RR-01192, EB002495 and AR47551), the Air Force Office of Scientific Research (FA9550-04-1-0101), and the Beckman Laser Institute Endowment.

W. Jung and Z. Chen are with the Beckman Laser Institute and the Department of Biomedical Engineering, University of California, Irvine, CA 92717 USA (e-mail: jungw@uci.edu; z2chen@uci.edu).

J. Zhang and J. Chung are with the Beckman Laser Institute, University of California, Irvine, CA 92717 USA.

P. Wilder-Smith is with the Beckman Laser Institute and the Department of Surgery, University of California, Irvine, CA 92717 USA.

M. Brenner is with the Beckman Laser Institute, University of California, Irvine, CA 92717 USA, and also with the Department of Pulmonary Medicine, University of California Medical Center, Orange, CA 92868 USA.

J. S. Nelson is with the Beckman Laser Institute, the Department of Biomedical Engineering, and the Department of Surgery, University of California, Irvine, CA 92717 USA.

Digital Object Identifier 10.1109/JSTQE.2005.857678

1077-260X/$20.00 © 2005 IEEE

small field of view and limited penetration depth considerably reduce the clinical usefulness of this approach. Therefore, the current approach to diagnosis is surveillance combined with biopsy or surgical excision. However, visual examination provides very poor diagnostic accuracy, and biopsy techniques are invasive, and unsuitable for regular screening of high risk sectors of the population.

Optical coherence tomography (OCT) is an imaging modality capable of providing noninvasive cross sectional imaging of biological tissue [11]–[13]. Frequently, OCT is compared to ultrasound imaging because both technologies employ backscattered signals reflected from different layers within the tissue to reconstruct structural images. In contrast to conventional medical imaging modalities, OCT provides images with high resolution (micrometer scale) in real time, and can be obtained noninvasively by the incorporation of OCT into flexible fiberoptic probes which enables minimally invasive imaging of a wide variety of organ systems. OCT has a wide range of potential applications in diagnosing diseases in various structures such as the eye, skin, gastrointestinal, respiratory, and genitourinary tracts, and the oral cavity [14]–[21]. OCT penetration depths are approximately 2–3 mm, enabling high resolution imaging of the surface and superficial tissues accessible by endoscopic probes. Our previous work showed that the imaging penetration depth of OCT is sufficient to evaluate macroscopic characteristics of epithelial and subepithelial structures with potential for near histopathological level resolution [22]. In addition, through statistical analysis between OCT images and corresponding histological sections, we demonstrated that it is possible to provide diagnostic information for precancerous lesions. This capability is primarily intended for regular monitoring of suspect lesions in the oral cavity and for rapid, low cost screening of high risk populations. In its early stages, the device's resolution or diagnostic capability may dictate its primary use as an indicator of the need for biopsy. However, in many cases, a 2-D image is not sufficient to fully visualize morphological features or to determine the margins of cancerous tissues. At more advanced stages of development, OCT may progressively further reduce the need for biopsy, to define surgical margins, and to provide a direct evaluation of the effectiveness of cancer treatments.

In the present study, we propose to develop a noninvasive clinical diagnostic capability for the oral cavity. The use of 2-D and expanded 3-D OCT for detection of oral cancer using an hamster cheek pouch model was investigated. Herein, we present conventional 2-D OCT, optical Doppler tomography (ODT), and 3-D volume images demonstrating detection of morphological changes during carcinogenesis in the hamster cheek pouch model and the enhanced capability of our 3-D approach.

## II. Materials and Methods

### A. Animal Model Preparation

A total 39 hamster cheek pouch (*Mesocricetus auratus*) specimens from female Golden Syrian were used. An application of 0.5% DMBA (9, 10 dimethyl-1, 2-benzanthracene) in mineral oil three times per week to the oral mucosa produced mild to severe dysplasia in 3–6 weeks, which progressed to squamous cell carcinoma at approximately 10 weeks. The median lining wall of one cheek pouch in each hamster was treated with DMBA carcinogen in mineral oil; the contralateral cheek pouch was treated only with mineral oil and served as control. Previous studies have shown that this carcinogenesis process in one cheek pouch does not affect the other cheek and, therefore, the untreated cheek pouch can be used as a control. Histological features in this model have been shown to correspond closely with premalignancy and malignancy in human oral mucosa.

Hamsters were placed in a chamber and inhalational anesthesia was administered. Half of the animals were further anesthetized with intraperitoneal 2:1 Ketamine HCL (100 mg/ml): Xylazine (20 mg/ml) at a dose of 0.75 cc/kg. The cheek pouches were everted, held in place with a fixation device, and imaged *in vivo*. After imaging, the hamsters were euthanized and the specimens excised for histologic preparation. Half of the animals were euthanized, and the cheek pouches were immediately removed and imaged *in situ* before histological processing [22], [23].

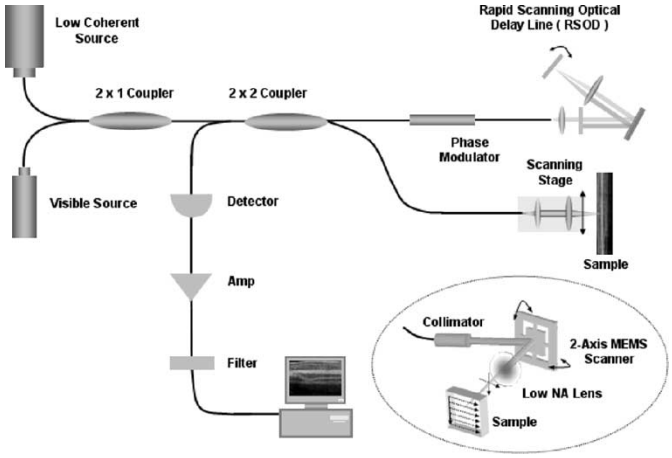


Fig. 1. Schematic of OCT imaging system: RSOD, rapid-scanning optical delay. Two kinds of beam delivery devices were used: One is a bench-top moving stage scanner with objective lens and collimator. Dotted line indicates the other, which is based on the 2-axis MEMS scanner and collimator. 3-D images are acquired when the MEMS mirror is integrated with the fiber based OCT system.

### B. OCT Instrumentation

Fig. 1 shows a schematic of the OCT system. Light was coupled into the interferometer and split into sample and reference beams. The OCT system used in this study employed a broadband super-luminescent diode laser light source that delivered an output power of 10 mW at a central wavelength of 1310 nm with a bandwidth of 70 nm. A visible aiming beam (633 nm) was used to locate the exact imaging position on the sample. In the reference arm, a rapid-scanning optical delay line was used that employed a grating to control the phase and group delays separately, so that no phase modulation is generated when the group delay was scanned [24], [25]. Phase modulation was generated through an electro-optic phase modulator that

produces a carrier frequency. The axial line scanning rate was 400 Hz, and the modulation frequency of the phase modulator was 500 kHz. Reflected beams from the two arms of the interferometer were recombined and detected on a photodetector. The interference signal was observed only when the optical path length difference between sample and reference arms was less than the coherence length of the source. The detected optical interference fringe intensity signals were bandpass filtered at the carrier frequency. Resultant signals were then digitized with an analog-digital converter, and transferred to a computer where the structural image was generated. The lateral and axial resolutions of the reconstructed image were 10 and 15 $\mu$m, respectively. To generate the 3-D volume images, a 2-D scanner based on an Si-MEMS mirror was integrated into the OCT system. Each 2-D cross-sectional image was acquired by one axis lateral scanning of the MEMS scanner sequentially after each axial scanning of the rapid scanning optical delay (RSOD), and continuously saved. Similarly, 3-D image sets were obtained by a combination of transverse scans, longitudinal scans by the MEMS scanner, and axial scans by the RSOD reference arm. Both transverse and the longitudinal scans by the MEMS scanner were synchronized with axial scanning of the RSOD. After recording, 3-D volume images were derived by software from the 3-D images.

### C. Measurements

For the *in situ* specimens, the cheek pouches were removed immediately after sacrifice and prepared for OCT imaging. The tissue was stretched over a flat cork surface and pinned using 0.20 mm insect pins. The cheek pouch surface was then covered with a thin layer of KY Gel (Johnson & Johnson Products, Inc, NJ) to prevent tissue desiccation during the imaging process. A visible He-Ne laser guide beam was used to position the samples for OCT acquisition on the stage. Triangular shaped notches were cut at opposite ends of the tissue to document the line of image acquisition. After imaging, tissue was formalin fixed and processed for paraffin embedding. Six micrometer paraffin sections were H&E stained and underwent histological evaluation. For the *in vivo* studies, cheek pouches were everted, clamped, and imaged *in vivo* and in near real time. Imaging was performed *in vivo* and in nearly real time. In some animals, imaging at the same location was performed twice to provide an indication of image fidelity. After imaging, animals were sacrificed and the tissue removed and processed for sectioning in the same manner as the *in situ* samples. OCT images for each tissue sample were compared with the corresponding histologic sections using a light microscope.

### D. Image Processing and Analysis

In Fig. 1, the dotted line indicates a schematic of the 3-D scanning methodology. The sequential 2-D images were continuously saved and displayed in real time during scanning. When the full 2-D scan was completed, the collected data was reconstructed to generate a 3-D volume image. Following data acquisition, the 3-D volume image was visualized using dedicated software providing image processing capabilities, such as isosurface extraction, filtering, thresholding, pseudocoloring, animation, and region selection. Then, 2-D image slices were generated at specific sites of interest. These images were amenable to manipulation and rotation at any angle by the clinician. 2-D OCT images were evaluated for the following criteria: changes in keratinization, epithelial thickening, epitherial proliferation and invasion, broadening of rete pegs, irregular epithelial stratification, and basal hyperplasia. Epithelial invasion was defined as a loss of the visible basement membrane. In the 3-D images, the ability to convey information of the same criteria was analyzed at multiple locations. Our clearly defined statistical approach to diagnosis, data quantification, and evaluation has been previously described and is not presented here [22].

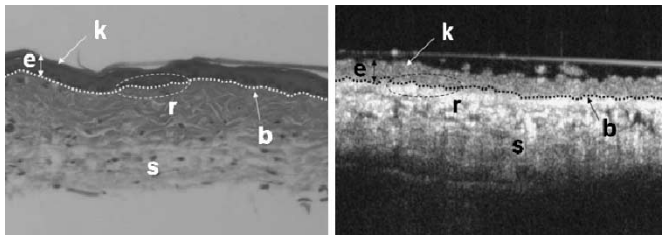


Fig. 2. Comparison between H&E section (left) and OCT image (right, 2 × 1.3 mm, 10 $\mu$m/pixel) of normal hamster cheek pouch: e, squamous epithelium; k, keratinized surface layer of epithelium; r, rete pegs; s, submucosa. The arrow indicates the basement membrane, b, in both images.

## III. Results and Discussion

Conventional 2-D OCT images with 10 $\mu$m axial resolution, 1.3 mm axial by variable lengths from 2–14 mm in the horizontal direction, were obtained. Fig. 2 shows a representative OCT image and corresponding histology of a normal hamster cheek pouch. The OCT images corresponded very closely to the standard histological light microscopic slides. Excellent resolution of tissue structures, such as surface keratinized layer, squamous epithelium, rete pegs, no basal hyperplasia, submucosa, and intact basement membrane were obtained and were easily recognizable due to their strong similarities to standard histology.

Fig. 3 depicts *in vivo* OCT and ODT images of a normal hamster cheek pouch. Surface and subsurface mucosal layers are evident. In Fig. 3(A), a blood vessel is seen in cross section. The same blood vessel is shown within the white dotted circle at higher magnification in Fig. 3(E). and 3(F) shows the color-coded blood velocity image of the same vessel demonstrating the ability of OCT/ODT to document *in vivo* the presence, dimensions, and perfusion of subsurface blood vessels. OCT/ODT imaging throughout carcinogenesis allows tracking of vascular and perfusion changes in individual blood vessels during the progression from normal through dysplasia to malignancy.

The ability of *in vivo* OCT to show mild dysplasia is demonstrated in Fig. 4. Epithelial thickening, broader rete pegs, moderate surface keratinolayer, and some basal membrane are visible. In Fig. 4(B)–(D), a thin keratinized epithelial layer is present above a thicker layer of flat, stratified squamous epithelium. The columnar basal cells are polarized and the underlying

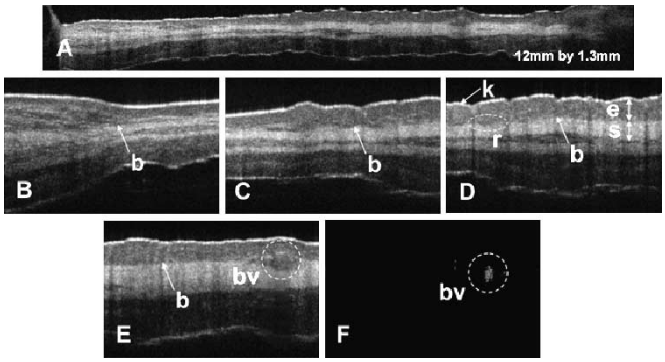


Fig. 3. *In vivo* OCT/ODT images of normal hamster cheek pouch: (A), a 12 mm segment of normal hamster cheek pouch obtained by OCT; (B)–(E), higher magnification views of Fig. 3(A). The size of OCT images (B)–(E) shown is $2 \times 1.3$ mm with 10 $\mu$m/pixel display resolution; F, velocity image of blood flow in the vessel shown in Fig. 3(E): bv, blood vessel; e, squamous epithelium; k, keratinized surface layer; r, rete pegs; s, submucosa. The arrow indicates the basement membrane, b.

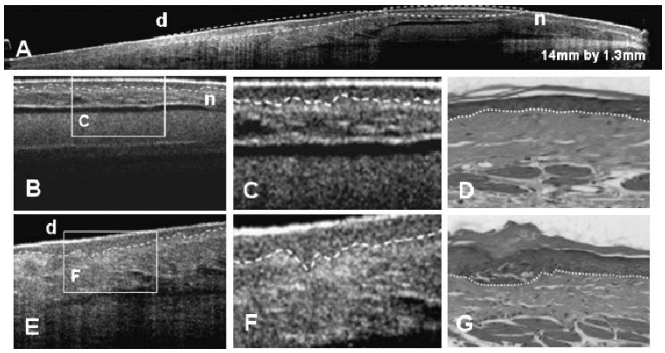


Fig. 4. *In vivo* OCT images of hamster cheek pouch with dysplasia: (A), a 14 mm segment of hamster cheek pouch with healthy dyplasia obtained by OCT: n, normal epithelial and subepithelial layer; d, area of dysplasia with epithelial down growth; (B)–(D), OCT image of normal hamster cheek pouch and corresponding histology; (E)–(G), OCT image of hamster cheek pouch with dysplasia and corresponding histology; (B), (E), higher magnification views of Fig. 4(A). The size of OCT images shown is $2 \times 1.3$ mm with 10 $\mu$m/pixel display resolution. (C) and (F), higher magnification views of Fig. 4(B), and (E). The location of basement membrane was indicated by the dotted lines.

basement membrane is fully intact. In the dysplasia region, Fig. 4(E)–(G), both the keratinized and squamous epithelial layers are thickened. The squamous epithelial cells show increased hyperchromatism, and there is decreased polarity in the basal layer adjacent to the basement membrane. The basement membrane remains intact. These observations correspond with similar features within H&E stain histopathological images shown in Fig. 4(D) and Fig. 4(G).

Fig. 5 depicts an OCT image of oral malignancy. The *in vivo* OCT image shows a thickened keratinized layer above the greatly thickened squamous epithelial layer. The squamous cells show increased hyperchromatism, pleomorphism of individual cells, and loss of polarity in the basal cell layer. The basement membrane is no longer intact and proliferating cells are invading the underlying submucosal connective tissue. This feature is correlated very well with corresponding histopathology seen in Fig. 5(D).

The images in Fig. 6 compare OCT and H&E images of a fungiform oral cancer. The epithelium is folded, as are the mucosa and basement membrane. The basement membrane is no longer intact due to epithelial invasion into the connective tissue below. Since OCT measures backscattering light intensity, the dark region, which corresponds to a reduced OCT signals, indicate that the backscattering coefficient is reduced. The cancerous tissue appears darker in the OCT image in part because it contains more blood than normal tissue. The OCT system used in these studies employs a 1300 nm light source. At this wavelength, light absorption by blood is considerable, which produces the darker appearance of the malignant tissue.

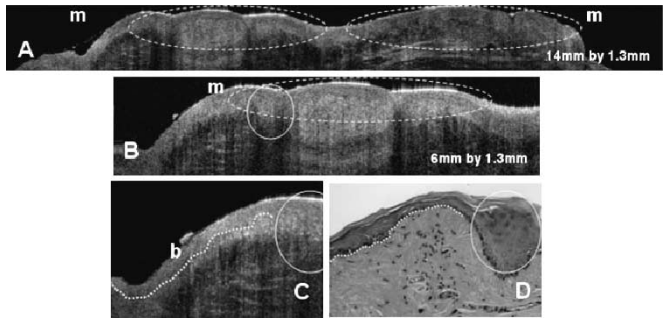


Fig. 5. *In vivo* OCT images of malignant hamster cheek pouch: (A), 14 mm segment of hamster cheek pouch obtained by OCT: m, malignant, b, base membrane; Fig. 5(B)–(C) are higher magnification views of Fig. 5(A). The size of OCT images (C) shown is $2 \times 1.3$ mm with 10 $\mu$m/pixel display resolution. In the image Fig. 5(C), basement membrane was outlined by a dotted line. (D), corresponding histology of OCT image in Fig. 5(C): Note the basement membrane is not continuously present in the area of malignancy and epithelium downgrowth and invasion are visible.

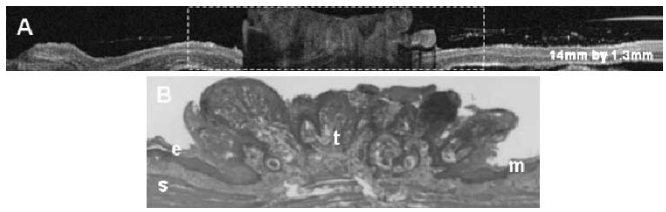


Fig. 6. *In vivo* OCT image and H&E section of hamster cheek pouch with fungiform cancer: (A), a 14 mm segment of hamster cheek pouch obtained by OCT; (B) shows H&E section corresponding dotted cancerous region in Fig. 6 (A): e, squamous epithelium; m, mucosa; s, submucosa, f, fungiform malignant. tissue.

Finally, Figs. 7 and 8 shows 3-D volume images of normal and abnormal hamster cheek pouch tissues. Since the threshold value was given by the intensity value on the images, the background was removed and only the tissue objects were visualized. Fig. 7 presents 3-D normal mucosal tissue structure with epithelium and mucosa. Resembling Fig. 3, Fig. 7 clearly shows thin normal epithelial and thick subepithelial layers in the corner of the 3-D image using a different viewing angles.

Fig. 8 presents *in vitro* 3-D OCT images of a hamster cheek pouch with squamous cell carcinoma. The cancerous and normal regions are marked by red and blue dotted circles, respectively. The randomly sliced 2-D OCT images in both the normal and cancerous regions are shown in Fig. 8(B) and (C). As these figures demonstrate, 2-D OCT imaging can be used to quantitatively image cross sectional structure of tissue; however, 3-D OCT enables mapping and visualization of architectural

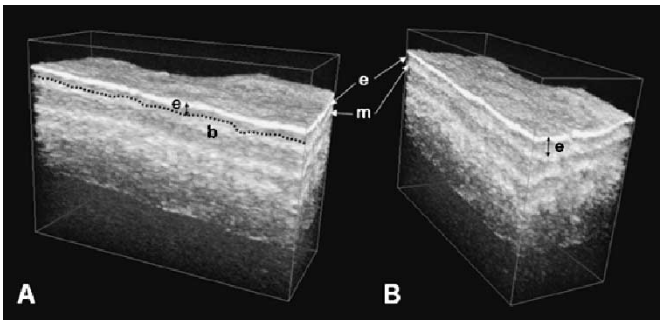


Fig. 7. *In vitro* 3-D OCT images of normal hamster cheek pouch: Image shows layered structure clearly: e, squamous epithelium; s, submucosa. The continuous base membrane line was visualized along the front and side view which was demonstrate with dot line. This phenomena was same in the different angled image.

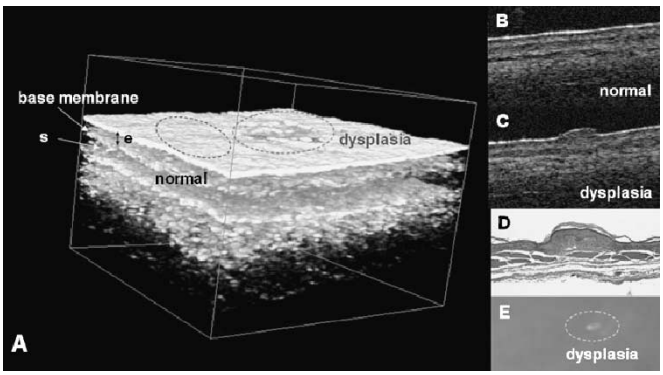


Fig. 8. (A), *In vitro* 3-D OCT images of hamster cheek pouch with cancer. Dysplasia and normal region are marked by the red dot and blue dot respectively. Image visualizes clear layered structure: e, squamous epithelium; s, submucosa: (B), 2-D OCT image in the normal tissue: (C)–(D), 2-D OCT image and corresponding histology in the cancerous region: (E), Microscopic image of hamster cheek pouch tissue. Dotted line indicates the cancerous region.

morphology. These advances in OCT imaging promise not only to improve the understanding of disease pathogenesis, but ultimately to enable earlier and more sensitive diagnosis, improve monitoring of disease progression, and allow assessment of cancer response to therapy.

OCT imaging has advantages that should be uniquely suitable for oral cancer evaluation, where near histologic level noninvasive detection and diagnosis of intraoral lesions will considerably improve the clinician's ability to detect such lesions. The feasibility of this concept was demonstrated in these studies using DMBA induced oral squamous cell carcinoma in a standard hamster cheek pouch model. Excellent resolution of dysplastic and malignant lesions was demonstrated, with close similarity between standard histologic data and *in vivo* OCT imaging. Alterations in epithelial structure, invasion of tissue boundaries, and other tissue characteristics of malignant transformation were clearly evident using OCT.

OCT is noninvasive, does not require ionizing radiation, and can be performed using relatively inexpensive diode laser based fiber-optic systems. Super luminescent diode light source based OCT systems are capable of obtaining 10–15 $\mu$m resolution. In the future, broader band light sources may enable resolutions approaching 1 $\mu$m. When such levels of resolution are achieved, nuclear characteristics may be distinguishable for *in vivo* optical cytologic level analysis of malignancy. Our ODT data demonstrated the ability to distinguish premalignant and malignant change in the oral mucosa. Furthermore, 3-D OCT images can provide additional information, such as delineating lesion margins or evaluating cancer response to therapy. Studies in patients with leukoplakia and early oral cancer are now under way to confirm these findings in humans, and to assess the capabilities of OCT for detecting and diagnosing human oral premalignancy and malignancy, and for screening and monitoring high risk patients.

## IV. Conclusion

We have successfully demonstrated the use of 2-D and 3-D OCT for early detection and diagnosis of oral premalignancy and malignancy. Our results demonstrate the feasibility of diagnostic imaging within the oral cavity using this modality. Noninvasive evaluation of neoplasia-related epithelial and subepithelial changes throughout carcinogenesis in the hamster cheek pouch model was achieved. OCT can clearly distinguish many histologic features such as epithelial and subepithelial change. 3-D images provide detailed structural information at any location, and may be viewed at any angle desired by the clinician. The appearance of structures imaged by OCT corresponded closely to histologic images. Given the ability to obtain high resolution images, flexible fiberoptic bronchoscopic compatibility, and *in vivo* noninvasive measurement, OCT has the potential to become a powerful method for early oral cancer detection.

## Acknowledgment

The authors acknowledge D. T. McCormick who provided 2 axis MEMS scanner for 3-D imaging. They also would like to thank M. Wilson, D. S. Mukai, N. El-Abbadi, N. Hanna, T. Waite-Kennedy, and T. Burney for their help with animal preparation, regulatory compliance, and sample processing.

## References

[1] *"Cancer Facts and Figures,"* American Cancer Society, New York, p.4, 2000.

[2] J. A. Regezi and J. Seinbba, "Oral Pathology," *WB Saunders Co*., pp. 77–90, 1993.

[3] T. Poate, J. Buchanan, T. Hodgson, P. Speight, A. Barrett, D. Moles, C. Scully, and S. Porter, "An audit of the efficacy of the oral brush biopsy technique in a specialist oral medicine unit," *Oral Oncol*., vol. 40, pp. 829–834, 2004.

[4] A. Acha, M. T. Ruesga, M. J. Rodriguez, M. A. Pancorbo, and J. M. Aguirre, "Applications of the oral scraped (exfoliative) cytology in oral cancer and precancer," *Oral Surg., Oral Med., Oral Pathol., Oral Radiol., Endodonto*., vol. 10, pp. 95–102, 2005.

[5] A. C. Jones, F. E. Pink, P. L. Sandow, C. M. Stewart, C. A. Migliorati, and R. A. Baughman, "The cytobrush plus cell collector in oral cytology," *Oral Surg. Oral Med. Oral Pathol*., vol. 77, pp. 95–99, 1994.

[6] I. J. Bigio and S. G. Bown, "Spectroscopic sensing of cancer and cancer therapy: Current status of translational research," *Cancer Biol. Ther.*, vol. 3, pp. 259–67, 2004.

[7] K. Sokolov, M. Follen, and R. Richards-Kortum, "Optical spectroscopy for detection of neoplasia," *Curr. Opin. Chem. Biol*., vol. 6, pp. 651–658, 2002.

[8] H. Inoue, T. Igari, T. Nishikage, K. Ami, T. Yoshida, and T. Iwai, "A novel method of virtual histopathology using laser-scanning confocal microscopy in-vitro with untreated fresh specimens from the gastrointestinal mucosa," *Endoscopy*, vol. 32, pp. 439–443, 2000.
[9] W. M. White, M. Rajadhyaksha, S. Gonzalez, R. L. Fabian, and R. R. Anderson, "Noninvasive imaging of human oral mucosa in vivo by confocal reflectance microscopy," *Laryngoscope*, vol. 109, pp. 1709–1717, 1999.
[10] A. M. Clark, A. M. Gillenwater, T. G. Collier, R. Alizadeh-Naderi, A. K. El-Naggar, and R. Richards-Kortum, "Confocal microscopy for real-time detection of oral cavity neoplasia," *Clin. Cancer Res.*, vol. 9, pp. 4714–4721, 2003.
[11] D. Huang, E. A. Swanson, C. P. Lin, J. S. Schuman, W. G. Stinson, W. Chang W, M. R. Hee, T. Flotte, K. Gregory, C. A. Puliafito, and J. G. Fujimoto, "Optical coherence tomography," *Science*, vol. 254, pp. 1178–1181, 1991.
[12] A. F. Fercher, "Optical coherence tomography," *J. Biomed. Opt.*, vol. 1, pp. 157–173, 1996.
[13] J. M. Schmitt, "Optical coherence tomography (OCT): A review," *IEEE J. Sel. Topics Quantum Electron.*, vol. 7, no. 2, pp. 931–935, 2001.
[14] J. A. Izatt, M. R. Hee, E. A. Swanson, C. P. Lin, D. Huang, J. S. Schuman, C. A. Puliafito, and J. G. Fujimoto, "Micrometer-scale resolution imaging of the anterior eye with optical coherence tomography," *Arch. Ophthamol.*, vol. 112, pp. 1584–1589, 1994.
[15] J. M. Schmitt, M. Yadlowsky, and R. F. Bonner, "Subsurface imaging if living skin with optical coherence tomography," *Dermatol.*, vol. 191, pp. 93–98, 1995.
[16] K. Kobayashi, J. A. Izatt, M. D. Kulkarni, J. Willis, and M. V. Sivak Jr., "High-resolution cross-sectional imaging of the gastrointestinal tract using optical coherence tomography: Preliminary results," *Gastrointest. Endosc.*, vol. 47, pp. 515–23, 1998.
[17] T. M. Yelbuz, M. A. Choma, L. Thrane, M. L. Kirby, and J. A. Izatt, "Optical coherence tomography: A new high-resolution imaging technology to study cardiac development in chick embryos," *Circulation*, vol. 106, pp. 2771–2774, 2002.
[18] G. J. Tearney, M. E. Brezinski, J. F. Southern, B. E. Bouma, S. A. Boppart, and J. G. Fujimoto, "Optical biopsy in human urologic tissue using optical coherence tomography," *J. Urol.*, vol. 157, pp. 1915–1919, 1997.
[19] B. W. Colston, M. J. Everett, L. B. Silva, L. L. Otis, P. Stroeve, and H. Nathel, "Imaging of hard and soft tissue structure in oral cavity by optical coherence tomography," *Appl. Opt.*, vol. 37, pp. 3582–3585, 1998.
[20] E. V. Zagaynova, O. S. Streltsova, N. D. Gladkova, L. B. Snopova, G. V. Gelikonov, F. I. Feldchtein, and A. N. Morozov, "In vivo optical coherence tomography feasibility for bladder disease," *J. Urol.*, vol. 167, pp. 1492–1496, 2002.
[21] C. Pitris, C. Jesser, S. A. Boppart, D. Stamper, M. E. Brezinski, and J. G. Fujimoto, "Feasibility of optical coherence tomography for high-resolution imaging of human gastrointestinal tract malignancies," *J. Gastroenterol.*, vol. 35, pp. 87–92, 2000.
[22] P. W. Smith, W. Jung, M. Brenner, K. Osann, H. Beydoun, D. Messadi, and Z. Chen, "In vivo optical coherence tomography for the diagnosis of oral malignancy," *Laser. Surg. Med.*, vol. 35, pp. 269–275, 2004.
[23] D. P. Slaughter, H. W. Southwick, and W. Smejkal, "Field cancerization in oral stratified squamous epithelium," *Cancer*, vol. 6, pp. 963–968, 1953.
[24] G. J. Tearney, B. E. Bouma, and F. G. Fujimoto, "High-speed phase—And group-delay scanning with a grating-based phase control delay line," *Opt. Lett.*, vol. 22, pp. 1811–1813, 1997.
[25] A. M. Rollins, M. D. Kulkarnis, S. Yazdanfar, R. Ung-arunyawee, and J. A. Izatt, "In vivo video rate optical coherence tomography," *Opt. Express*, vol. 3, pp. 219–229, 1998.

**Woonggyu Jung** received the B.S. degree in electronics engineering from the Kyungnam University, South Korea and the M.S. degree in sensor engineering from the Kyungpook National University, South Korea, in 1999 and 2001, respectively. He is currently working in the Beckman Laser Institute and toward the Ph.D. degree in biomedical engineering, University of California, Irvine.

His research interests include 3-D optical coherence tomography, endoscopic probe and optical MEMS device.

**Jun Zhang** received the Ph.D. degree on optics from Shanghai Jiaotong University, China, in 2001.

He joined as a Postdoctoral Researcher of the Beckman Laser Institute at University of California, Irvin, in 2002.

His research is focused on the development of optical coherence tomography (OCT), Fourier domain optical coherence tomography (FDOCT), optical Doppler tomography (ODT) and polarization sensitive optical coherence tomography (PS-OCT).

**Jungrae Jung** received the B.S. degree in biomedical engineering, the M.S. degree in electronics engineering from YonSei University, Korea, in 1985 and 1987, respectively, and the Ph.D. degree in biomedical engineering from Texas A&M University, College Station, in 2003.

From 1987 to 1998, she was a Researcher in the Research Center for Wireless Communication at SK Telecom Inc., a Korean wireless communication service provider, where she was a radio-frequency design engineer. Immediately after her Ph.D. degree, she joined Beckman Laser Institute at the University of California, Irvine, as a Postdoctoral Fellow and is engaged in biomedical projects exploring the light tissue interaction using polarized light scattering techniques. Her interests include the use of spectroscopy for the detection of precancerous changes *in vivo,* development of the theoretical approaches to describe light propagation in biological media, and biomedical instrumentation.

**Petra Wilder-Smith** is an Associate Professor and Director of Dentistry at the Beckman Laser Institute and Medical Clinic, University of California, Irvine. She is also Adjunct Assistant Professor at Loma Linda University Dental School, and Visiting Professor at Aachen University in Germany. She has been working with lasers since 1985, and is interested in imaging, diagnostic and therapeutic applications of lasers. Current projects include noninvasive diagnosis of premalignancy and malignancy, noninvasive imaging and diagnostics of biofilms, holographic measurement and "impression" techniques, noninvasive detection of periodontal disease activity, applications of lasers in endodontics and periodontics, and photodynamic diagnosis and therapy of biofilms and of malignancy. She has pioneered the noninvasive measurement of pulpal and periodontal blood flow and its relation to clinical and therapeutic parameters.

Dr. Wilder-Smith is an Honorary Fellow of UCI Cancer Center.

**Matt Brenner** received the M.D. degree from the University of California (UC), San Diego, in 1981.

He joined UC Irvine and the Beckman Laser Institute as a Faculty Member in 1988 after internal medicine residency at UC San Diego, and fellowship training in Critical Care Medicine at the National Institutes of Health, and Pulmonary Medicine at UC Irvine. He is currently a Professor of Medicine and Chief of the Pulmonary Division at UC Irvine and holds a joint faculty appointment in the Department of Surgery with the Beckman Laser Institute. His research interests involve translation of optical diagnostic technologies to medical applications in pulmonary and critical care fields. His group has demonstrated feasibility of using high-resolution optical coherence technology for airway

diagnostics in inhalation injury and cancer detection in animal models and patients. In addition, his group has developed animal models for assessing noninvasive optical methods for detection and monitoring of tissue perfusion and oxygenation using diffuse optical spectroscopy in animal models.

**J. Stuart Nelson** received the M.D. and Ph.D. degrees.

He is a Professor of Surgery, Dermatology and Biomedical Engineering, University of California, Irvine, and Associate Director of the Beckman Laser Institute and Medical Clinic.

The principal goal of his research has been to integrate experimental and theoretical descriptions of light propagation in homogeneous and heterogeneous biological tissues to yield a basis for dosimetry of laser-tissue interactions. He is particularly interested in addressing the problems associated with light propagation and dosimetry in human skin.

**Zhongping Chen** (M'03) received the Ph.D. degree in applied physics from Cornell University, Ithaca, NY, in 1992.

He joined the Beckman Laser Institute, University of California, Irvine, in 1995 and is currently a Professor of Biomedical Engineering at UC, Irvine. He also holds a joint faculty appointment in the Department of Electrical Engineering and Computer Science and Department of Surgery. He has published more than 70 peer-reviewed papers and review articles and holds a number of patents in the fields of biomaterials, biosensors, and biomedical imaging. His research interests encompass the areas of biomedical photonics, microfabrication, biomaterials, and biosensors. His group has developed a noninvasive technology, known as phase resolved functional optical coherence tomography, which allows cross-sectional imaging of tissue structure, blood flow, and birefringence simultaneously with high spatial resolution. His current research focuses on integrating advanced optical and microfabrication technology with biotechnology for the development of biomedical diagnostic and therapeutic devices.

Dr. Chen is a fellow of American Institute of Medical and Biomedical Engineering.